

# Probing the Excited States of d<sup>6</sup> Metal Complexes Containing the 2,2'-Bipyrimidine Ligand Using Time-Resolved Infrared Spectroscopy.

## 1. Mononuclear and Homodinuclear Systems

Wassim Z. Alsendi,<sup>†</sup> Timothy L. Easun,<sup>‡</sup> X.-Z. Sun,<sup>†</sup> Kate L. Ronayne,<sup>§</sup> Michael Towrie,<sup>§</sup> Juan-Manuel Herrera,<sup>‡</sup> Michael W. George,<sup>\*†</sup> and Michael D. Ward<sup>\*‡</sup>

School of Chemistry, University of Nottingham, University Park, Nottingham NG7 2RD, U.K., Department of Chemistry, University of Sheffield, Sheffield S3 7HF, U.K., and Central Laser Facility, CCLRC Rutherford Appleton Laboratory, Chilton, Didcot, Oxfordshire OX11 0QX, U.K.

Received December 4, 2006

This paper reports time-resolved infrared (TRIR) spectroscopic studies on a series of weakly luminescent or nonluminescent 2,2'-bipyrimidine-based complexes to probe their electronic structure and the dynamic behavior of their excited states on the picosecond and nanosecond time scales. The complexes are mononuclear [Re(CO)<sub>3</sub>Cl-(bpm)] (1), [Ru(CN)<sub>4</sub>(bpm)]<sup>2-</sup> (2), and [Ru(bpyam)<sub>2</sub>(bpm)]<sup>2+</sup> (3) [bpm = 2,2'-bipyrimidine; bpyam = 2,2'-bipyridine-4,4'-(CONEt<sub>2</sub>)<sub>2</sub>] and their homodinuclear analogues [{Re(CO)<sub>3</sub>Cl}<sub>2</sub>(μ-bpm)] (4), [{Ru(CN)<sub>4</sub>]<sub>2</sub>(μ-bpm)]<sup>2-</sup> (5), and [{Ru(bpyam)<sub>2</sub>]<sub>2</sub>(μ-bpm)]<sup>4+</sup> (6). Complex 1 shows the characteristic shift of the three ν(CO) bands to higher energy in the Re → bpm triplet metal-to-ligand charge-transfer (<sup>3</sup>MLCT) state, which has a lifetime of 1.2 ns. In contrast, the dinuclear complex 4 shows ν(CO) transient bands to both higher and lower energy than the ground state indicative of, on the IR time scale, an asymmetric excited state [(OC)<sub>3</sub>ClRe<sup>I</sup>(bpm<sup>•-</sup>)Re<sup>II</sup>(CO)<sub>3</sub>Cl] whose lifetime is 46 ps. The cyanoruthenate complexes 2 and 5 show comparable behavior, with a shift of the ν(CN) bands to higher energy in the excited state for mononuclear 2 but two sets of transient bands—one to higher energy and one to lower energy—in dinuclear 5, consistent with an asymmetric charge distribution [(NC)<sub>4</sub>Ru<sup>I</sup>(bpm<sup>•-</sup>)Ru<sup>III</sup>(CN)<sub>4</sub>]<sup>4-</sup> in the <sup>3</sup>MLCT state. These cyanoruthenate complexes have much longer lifetimes in D<sub>2</sub>O compared with CH<sub>3</sub>CN, viz., 250 ps and 3.4 ns for 2 and 65 ps and 1.2 ns for 5 in CH<sub>3</sub>CN and D<sub>2</sub>O, respectively. In complex 3, both higher-energy Ru → bpyam and lower-energy Ru → bpm <sup>3</sup>MLCT states are formed following 400 nm excitation; the former decays rapidly (τ = 6–7 ps) to the latter, and the subsequent decay of the Ru → bpm <sup>3</sup>MLCT state occurs with a lifetime of 60 or 97 ns in D<sub>2</sub>O or CH<sub>3</sub>CN, respectively. Similar behavior is shown by dinuclear 6 in both D<sub>2</sub>O and CH<sub>3</sub>CN, with initial interconversion from the Ru → bpyam to the Ru → bpm <sup>3</sup>MLCT state occurring with τ ~ 7 ps and the resultant Ru → bpm <sup>3</sup>MLCT state decaying on the nanosecond time scale.

### Introduction

Metal polypyridyl complexes that exhibit luminescence from charge-transfer excited states have been popular targets for investigation, with a wide range of potential applications such as solar energy harvesting,<sup>1</sup> catalysis<sup>2</sup> (both photochemical<sup>2a–c</sup> and electrochemical<sup>2f</sup>), sensors,<sup>3</sup> materials for molecular electronics and photonics,<sup>4</sup> and electroluminescent display devices,<sup>5</sup> making this an area of considerable current

interest. Understanding the photoinduced processes occurring within such metal complexes is of immense importance: not just the ultimate events such as photoinduced electron transfer or luminescence, which give the compounds their useful function, but the very early stage behavior of the excited state before the lowest-energy triplet metal-to-ligand charge-transfer (<sup>3</sup>MLCT) state is reached. Thus, very recent studies on ruthenium(II) polypyridyl complexes have involved both

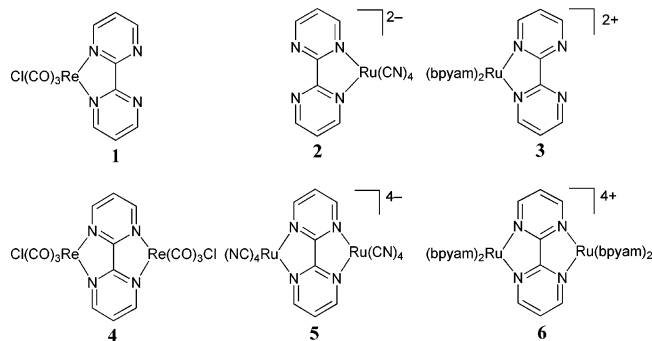
\* To whom correspondence should be addressed. E-mail: mike.george@nott.ac.uk (M.W.G.), m.d.ward@sheffield.ac.uk (M.D.W.).

<sup>†</sup> University of Nottingham.

<sup>‡</sup> University of Sheffield.

<sup>§</sup> CCLRC Rutherford Appleton Laboratory.

(1) (a) Alstrum-Acevedo, J. H.; Brennaman, M. K.; Meyer, T. J. *Inorg. Chem.* **2005**, *44*, 6802. (b) Grätzel, M. *Inorg. Chem.* **2005**, *44*, 6841. (c) Meyer, G. J. *Inorg. Chem.* **2005**, *44*, 6852. (d) Chakraborty, S.; Wadas, S.; Hester, H.; Schmehl, R.; Eisenberg, R. *Inorg. Chem.* **2005**, *44*, 6865.

**Chart 1.** Three Mononuclear Model Complexes (Top) and Their Homodinuclear Analogues (Bottom) Examined in This Study [bpyam = 2,2'-bipyrimidine-4,4'-(CONEt<sub>2</sub>)<sub>2</sub>]

extremes of the time scale: dyads in which photoinduced charge separation is very long-lived at one extreme<sup>6</sup> and ultrafast studies on the excited-state behavior of [Ru(bpy)<sub>3</sub>]<sup>2+</sup> before thermal equilibrium is reached at the other.<sup>7</sup> An important aspect of metal polypyridyl complexes is that there is a particularly clear relationship between structure and electronic properties, and accordingly synthetically straightforward control of the steric or electronic properties of the ligands can be used to fine-tune the photophysical properties of the complexes.<sup>8</sup>

In this paper, we describe studies on a series of three homodinuclear complexes of 2,2'-bipyrimidine (bpm) and their mononuclear analogues (Chart 1). Bpm has been and remains a popular bridging ligand in the study of polynuclear complexes, affording short metal–metal separations (ca. 5.5 Å) and strong electronic coupling between metal centers,<sup>9</sup> and there have been a number of studies on the photophysics and electrochemistry of such complexes.<sup>10,11</sup> Luminescence-

based photophysical studies on transition-metal complexes of bpm with d<sup>6</sup> metal ions such as rhenium(I) and ruthenium(II) have been limited by the fact that the excited states can be dark or only very weakly luminescent in room temperature solution compared to analogous complexes with 2,2'-bipyridine, with the dinuclear complexes having even weaker luminescence with shorter lifetimes compared with their mononuclear analogues.<sup>10</sup> Generally, there are several MLCT absorptions in these complexes, consistent with a greater number of molecular orbitals (MOs) available to participate in photophysical processes compared to bpy complexes, and the lowest MLCT absorption occurs at a longer wavelength than that in the corresponding bpy compounds,<sup>10</sup> consistent with the bpm lowest unoccupied MO (LUMO) being lower in energy than the bpy LUMO. The complexation of a second metal center to the bipyrimidine shifts the absorption bands to longer wavelengths, as the highest occupied MO (HOMO)–LUMO gap is decreased. Complexes of bpm containing the ReCl(CO)<sub>3</sub> moiety have been found to be either very weakly luminescent or nonluminescent at room temperature.<sup>10a,c</sup> Characteristic MLCT emission has been detected and characterized for [Ru(bpy)<sub>2</sub>-(bpm)]<sup>2+</sup>, with a lifetime of 76 ns in MeCN.<sup>10b</sup> Emission has only been reported for the solid at 77 K<sup>10b</sup> for the corresponding dinuclear complex, {[Ru(bpy)<sub>2</sub>]<sub>2</sub>(μ-bpm)}<sup>4+</sup>.

Our studies have been performed using the technique of time-resolved infrared (TRIR) spectroscopy<sup>12,13</sup> to probe both the nature and dynamic behavior of the excited states of the complexes. The complexes all contain IR-sensitive functional groups, either directly coordinated to the metal center (carbonyl and cyanide) or pendant from a terminal bpy ligand (amide and carbonyl), as spectroscopic handles to probe the nature of these states directly. The TRIR method has the advantage over luminescence-based methods for these complexes because of their generally weak luminescence, as

- (2) (a) Bossmann, S. H.; Turro, C.; Schnabel, C.; Pokhrel, M. R.; Payawan, L. M.; Baumeister, B.; Wörner, M. *J. Phys. Chem. B* **2001**, *105*, 5374. (b) Gholamkhass, B.; Mametsuka, H.; Koike, K.; Tanabe, T.; Furue, M.; Ishitani, O. *Inorg. Chem.* **2005**, *44*, 2326. (c) Baffert, C.; Dumas, S.; Chauvin, J.; Lepretre, J. C.; Collomb, M. N.; Deronzier, A. *Phys. Chem. Chem. Phys.* **2005**, *7*, 202. (d) Suzuki, M.; Waraska, C. C.; Mallouk, T. E.; Nakayama, H.; Hanabusa, K. *J. Phys. Chem. B* **2002**, *106*, 4227. (e) Hara, M.; Lean, J. T.; Mallouk, T. E. *Chem. Mater.* **2001**, *13*, 4668. (f) Deronzier, A.; Moutet, J.-C. In *Comprehensive Coordination Chemistry*, 2nd ed.; Ward, M. D., Ed.; Elsevier: Oxford, U.K., 2004; Vol. 9, p 471.
- (3) (a) Demas, J. N.; DeGraff, B. A. *Coord. Chem. Rev.* **2001**, *211*, 317. (b) Keefe, M. H.; Benkstein, K. D.; Hupp, J. T. *Coord. Chem. Rev.* **2000**, *205*, 201. (c) Cajlakovic, M.; Bizzarri, A.; Ribitsch, V. *Anal. Chim. Acta* **2006**, *573*, 57. (d) McGauhey, O.; Ros-Lis, J. V.; Guckian, A.; McEvoy, A. K.; McDonagh, C.; MacCraith, B. D. *Anal. Chim. Acta* **2006**, *570*, 15. (e) Holmlin, R. E.; Stemp, E. D. A.; Barton, J. K. *Inorg. Chem.* **1998**, *37*, 29. (f) Olson, E. J. C.; Hu, D.; Hormann, A.; Jonkman, A. M.; Arkin, M. R.; Stemp, E. D. A.; Barton, J. K.; Barbara, P. F. *J. Am. Chem. Soc.* **1997**, *119*, 11458.
- (4) (a) Coe, B. J.; Curati, N. R. M. *Comments Inorg. Chem.* **2004**, *25*, 147. (b) Low, P. J. *Dalton Trans.* **2005**, 2821. (c) Ziessel, R.; Hissler, M.; El-Ghayoury, A.; Harriman, A. *Coord. Chem. Rev.* **1998**, *178*, 1251. (d) Balzani, V.; Juris, A.; Venturi, M.; Campagna, S.; Serroni, S. *Chem. Rev.* **1996**, *96*, 759. (e) Benniston, A. C. *Chem. Soc. Rev.* **2004**, *33*, 573.
- (5) Evans, R. C.; Douglas, P.; Winscom, C. J. *Coord. Chem. Rev.* **2006**, *250*, 2093.
- (6) Borgström, M.; Shaikh, N.; Johansson, O.; Anderlund, M. F.; Styring, S.; Åkermark, B.; Magnuson, A.; Hammarström, L. *J. Am. Chem. Soc.* **2005**, *127*, 17504.
- (7) McFarland, S. A.; Lee, F. S.; Cheng, K. A. W. Y.; Cozens, F. L.; Schepp, N. P. *J. Am. Chem. Soc.* **2005**, *117*, 7065.
- (8) Juris, A.; Balzani, V.; Barigelletti, F.; Campagna, S.; Belser, P.; von Zelewsky, A. *Coord. Chem. Rev.* **1988**, *84*, 85.

- (9) (a) Herrera, J.-M.; Pope, S. J. A.; Adams, H.; Faulkner, S.; Ward, M. D. *Inorg. Chem.* **2006**, *45*, 3895. (b) Real, J. A.; Gaspar, A. B.; Muñoz, M. C.; Gutlich, P.; Ksenofontov, V.; Spiering, H. *Top. Curr. Chem.* **2004**, *233*, 167.
- (10) (a) Vogler, A.; Kisslinger, J. *Inorg. Chim. Acta* **1986**, *115*, 193. (b) Sahai, R.; Rillema, D. P.; Shaver, R.; Wallendaal, S. V.; Jackman, D. C.; Boldaji, M. *Inorg. Chem.* **1989**, *28*, 1022. (c) Matheis, W.; Kaim, W. *Inorg. Chim. Acta* **1991**, *181*, 15. (d) Shaver, R.; Perkovic, M. W.; Rillema, D. P.; Woods, C. *Inorg. Chem.* **1995**, *34*, 5446.
- (11) (a) Kaim, W.; Kohlmann, S.; Lees, A. J.; Snoeck, T. L.; Stufkens, D. J.; Zulu, M. M. *Inorg. Chim. Acta* **1993**, *210*, 159. (b) Kaim, W. *Inorg. Chem.* **1984**, *23*, 3365. (c) Dodswoth, E. S.; Lever, A. B. P. *Coord. Chem. Rev.* **1990**, *97*, 271. (d) Kaim, W.; Kohlmann, S. *Inorg. Chem.* **1986**, *25*, 3306. (e) van Outersterp, J. W. M.; Stufkens, D. J.; Vlcek, A. *Inorg. Chem.* **1995**, *34*, 5183.
- (12) (a) Turner, J. J.; George, M. W.; Johnson, F. P. A.; Westwell, J. R. *Coord. Chem. Rev.* **1993**, *125*, 101. (b) Schoonover, J. R. S.; Strouse, G. F. *Chem. Rev.* **1998**, *98*, 1335. (c) George, M. W.; Turner, J. J. *Coord. Chem. Rev.* **1998**, *177*, 201. (d) Kuimova, M. K.; Gordon, K. C.; Howell, S. L.; Matousek, P.; Parker, A. W.; Sun, X. Z.; George, M. W. *Photochem. Photobiol. Sci.* **2006**, *5*, 82. (e) Gabriellsson, A.; Hartl, F.; Zhang, H.; Smith, J. R. L.; Towrie, M.; Vlcek, A.; Perutz, R. N. *J. Am. Chem. Soc.* **2006**, *128*, 4253. (f) Blanco-Rodriguez, A. M.; Busby, M.; Gradinaru, C.; Crane, B. R.; Di Bilio, A. J.; Matousek, P.; Towrie, M.; Leigh, B. S.; Richards, J. H.; Vlcek, A.; Gray, H. B. *J. Am. Chem. Soc.* **2006**, *128*, 4365. (g) Kovenov, Y. A.; Blake, A. J.; George, M. W.; Matousek, P.; Mel'nikov, M. Y.; Parker, A. W.; Sun, X. Z.; Towrie, M.; Weinstein, J. A. *Dalton Trans.* **2005**, 2092. (h) Portius, P.; Yang, J. X.; Sun, X. Z.; Grills, D. C.; Matousek, P.; Parker, A. W.; Towrie, M.; George, M. W. *J. Am. Chem. Soc.* **2004**, *126*, 10713.

mentioned above. We were particularly interested in three features of the complexes. First, the lowest-energy MLCT excited states of the symmetrical dinuclear complexes  $M-bpm-M$  could be either localized at one metal center ( $M^+-L^-M$  as the limiting description) or delocalized equally over both ( $M^{0.5+}-L^-M^{0.5+}$ ) on the IR time scale.<sup>14,15</sup> Second, complexes **3** and **6**, in which there are both bpy and bpm ligands capable of participating in MLCT excited states, can undergo excitation to either  $Ru \rightarrow bpm$  or  $Ru \rightarrow bpy$  MLCT states. Knowledge of the localization and rate of formation of the lowest MLCT state in heteroleptic ruthenium(II) complexes is important for understanding subsequent processes such as photoinduced energy or electron transfer to quencher groups or electron injection into dye-sensitized solar cells from nonexcited states above the lowest MLCT level.<sup>16</sup> Third, the cyanoruthenate complexes **2** and **5** belong to a family whose members show strong solvatochromism associated with interactions of the cyanide lone pairs with protic solvents,<sup>17</sup> and we were interested in examining the excited-state dynamics and TRIR behavior of these as a function of the solvent.

## Experimental Section

**Syntheses.** 2,2'-Bipyrimidine was purchased from Aldrich and used as received. Potassium hexacyanoruthenate trihydrate was provided on loan by Johnson Matthey plc. Rhenium pentacarbonyl chloride was purchased from Alfa Aesar and used as received. <sup>1</sup>H NMR spectra were recorded on a Bruker AC 250 spectrometer, and all mass were recorded on a VG AutoSpec magnetic sector instrument.

- (13) (a) Whittle, C. E.; Weinstein, J. A.; George, M. W.; Schanze, K. S. *Inorg. Chem.* **2001**, *40*, 4053. (b) Cooper, T. M.; Blaudeau, J. P.; Hall, B. C.; Rogers, J. E.; McLean, D. G.; Liu, Y. L.; Toascano, J. P. *Chem. Phys. Lett.* **2004**, *400*, 239. (c) Emmert, L. A.; Choi, W.; Marshall, J. A.; Yang, J.; Meyer, L. A.; Brozik, J. A. *J. Phys. Chem.* **2003**, *107*, 11340. (d) Weinstein, J. A.; Blake, A. J.; Davies, E. S.; Davis, A. L.; George, M. W.; Grills, D. C.; Lileev, I. V.; Maksimov, A. M.; Matousek, P.; Mel'nikov, M. Y.; Parker, A. W.; Platonov, V. E.; Towrie, M.; Wilson, C.; Zheligovskaya, N. N. *Inorg. Chem.* **2003**, *42*, 7077. (e) Kuimova, M. K.; Mel'nikov, M. Y.; Weinstein, J. A.; George, M. W. *J. Chem. Soc., Dalton Trans.* **2002**, 2857. (f) Encinas, S.; Morales, A. F.; Barigelletti, F.; Barthram, A. M.; White, C. M.; Couchman, S. M.; Jeffery, J. C.; Ward, M. D.; Grills, D. C.; George, M. W. *J. Chem. Soc., Dalton Trans.* **2001**, 3312.
- (14) (a) Plummer, E. I.; Zink, J. I. *Inorg. Chem.* **2006**, *45*, 6556. (b) Lockard, J. V.; Zink, J. I.; Konradsson, A. E.; Weaver, M. N.; Nelsen, S. F. *J. Am. Chem. Soc.* **2003**, *125*, 13471.
- (15) (a) Abbott, L. C.; Arnold, C. J.; Ye, T. Q.; Gordon, K. C.; Perutz, R. N.; Hester, R. E.; Moore, J. N. *J. Phys. Chem. A* **1998**, *102*, 1252. (b) Kuimova, M. K.; Gordon, K. C.; Howell, S. L.; Matousek, P.; Parker, A. W.; Sun, X.-Z.; Towrie, M.; George, M. W. *Photochem. Photobiol. Sci.* **2006**, *5*, 82. (c) Omberg, K. M.; Schoonover, J. R.; Meyer, T. J. *J. Phys. Chem. A* **1997**, *101*, 9531. (d) Ortiz, T. P.; Marshall, J. A.; Emmert, L. A.; Yang, J.; Choi, W.; Costello, A. L.; Brozik, J. A. *Inorg. Chem.* **2004**, *43*, 132. (e) George, M. W.; Johnson, F. P. A.; Turner, J. J.; Westwell, J. R. *J. Chem. Soc., Dalton Trans.* **1995**, 2711. (f) Dattelbaum, D. M.; Hartshorn, C. M.; Meyer, T. J. *J. Am. Chem. Soc.* **2002**, *124*, 4938.
- (16) (a) Constable, E. C.; Handel, R. W.; Housecroft, C. E.; Morales, A. F.; Flamigni, L.; Barigelletti, F. *Dalton Trans.* **2003**, 1220. (b) Schoonover, J. R.; Dattelbaum, D. M.; Malko, A.; Klimov, V. I.; Meyer, T. J.; Styers-Barnett, J.; Gannon, E. Z.; Granger, J. C.; Aldridge, W. S.; Papanikolas, J. M. *J. Phys. Chem. A* **2005**, *109*, 2472. (c) Omberg, K. M.; Smith, G. D.; Kavallunas, D. A.; Chen, P.; Treadway, P.; Schoonover, J. R.; Palmer, R. A.; Meyer, T. J. *Inorg. Chem.* **1999**, *38*, 951. (d) Liu, F.; Meyer, G. J. *Inorg. Chem.* **2005**, *44*, 9305. (e) Houarner, C.; Blart, E.; Buvat, P.; Odobel, F. *Photochem. Photobiol. Sci.* **2005**, *4*, 200. (f) Glazer, E. C.; Magde, D.; Tor, Y. J. *Am. Chem. Soc.* **2005**, *127*, 4190.
- (17) Ward, M. D. *Coord. Chem. Rev.* **2006**, *250*, 3128.
- The compounds  $[Re(bpm)(CO)_3Cl]$  (**1**),<sup>10a</sup>  $[Cl(CO)_3Re(\mu-bpm)-Re(CO)_3Cl]$  (**4**),<sup>10a</sup>  $[Ru(bpm)(CN)_4]^{2-}$  (**2**),<sup>18a</sup> and  $[Ru(CN)_4]_2(\mu-bpm)]^{4-}$  (**5**)<sup>18b</sup> were made according to previously published procedures (counteractions for the anionic complexes **2** and **5** were  $K^+$  for studies in  $D_2O$  and  $PPN^+$  for studies in  $CH_3CN$ ). The ligand 2,2'-bipyridine-4,4'-(CONEt<sub>2</sub>)<sub>2</sub> (hereafter abbreviated as bpyam) was also prepared according to a published procedure.<sup>19</sup>
- (a) Synthesis of  $Ru(bpyam)_2Cl_2$ .** A mixture of  $RuCl_3 \cdot 3H_2O$  (2.62 g, 10.0 mmol), LiCl (3.25 g, 77 mmol, a large excess), and bpyam (6.83 g, 19.2 mmol) was refluxed with stirring in dry *N,N*-dimethylformamide (DMF; 200 mL) for 20 h to give a brown solution. The solvent was distilled off, the residue dissolved in  $CH_2Cl_2$ , and the solid filtered off. The solution was extracted with copious water ( $5 \times 1$  L) to remove any orange, water-soluble  $[Ru(bpyam)_3]Cl_2$ . The remaining  $CH_2Cl_2$  solution was evaporated to dryness and the purple product purified by column chromatography on silica with  $CH_2Cl_2/CH_3OH$  (10:1, v/v) as the eluant to give the desired product as a purple solid (6.11 g, 72%). ESMS:  $m/z$  845  $\{M - Cl\}^+$  (calcd 845.3). <sup>1</sup>H NMR (250 MHz,  $CDCl_3$ ):  $\delta$  1.1–1.3 (24 H, m;  $CH_3$ ), 3.3–3.6 (16 H, m;  $CH_2$ ), 6.92 (2 H, d,  $J = 5.8$  Hz;  $H^6$ ), 7.56 (2 H, d,  $J = 5.8$  Hz;  $H^5$ ), 7.64 (2 H, d,  $J = 5.8$  Hz;  $H^5$ ), 8.03 (2 H, d,  $J = 1.3$  Hz;  $H^3$ ), 8.19 (2 H, d,  $J = 1.3$  Hz;  $H^3$ ), 10.36 (2 H, d,  $J = 5.8$  Hz;  $H^6$ ).
- (b) Synthesis of  $[(bpyam)_2Ru(bpm)]Cl_2$  (**3**) and  $[(bpyam)_2Ru]_2(\mu-bpm)]Cl_4$  (**6**).** Bipyrimidine (0.45 g, 2.8 mmol) and  $Ru(bpyam)_2Cl_2$  (2.99 g, 3.4 mmol) were combined in ethanol (110 mL), and the mixture was heated to reflux for 50 h to form a red-brown solution. After cooling to room temperature, the solvent was evaporated off. The products were separated by column chromatography on Sephadex SP C-25, eluting with aqueous NaCl. Initial use of water eluted unreacted  $Ru(bpyam)_2Cl_2$ . Use of 0.1 M NaCl resulted in the elution of red mononuclear **3**, the major product. Increasing the NaCl concentration to 0.4 M then resulted in the elution of small quantities of green-red dinuclear **6**. For each fraction, the solvent was evaporated and the product dissolved in  $CH_2Cl_2$  and filtered to remove NaCl. Evaporation of  $CH_2Cl_2$  yielded red solid **3** (yield 57%) and dark green-red solid **6** (yield 2%).
- Data for **3**. Anal. Calcd for  $[(bpyam)_2Ru(bpm)]Cl_2 \cdot 6H_2O$  (**3**): C, 50.2; H, 6.2; N, 14.7. Found: C, 49.9; H, 5.7; N, 14.8. FABMS:  $m/z$  1003  $[M - Cl]^+$  (calcd 1003.6), 967  $[M - 2Cl]^+$  (calcd 968.4). ESMS:  $m/z$  484  $[M - 2Cl]^{2+}$  (calcd 484.2).
- Data for **6**. ESMS:  $m/z$  924  $[M - 2Cl]^{2+}$  (calcd 924.3), 444  $[M - 4Cl]^{4+}$  (calcd 444.7).
- Spectroscopic, Luminescence, and Electrochemistry Studies.** Fourier transform infrared (FTIR) spectra were recorded in standard  $CaF_2$  solution cells (Specac) using a Nicolet Avatar 360 FTIR spectrometer, typically at  $2\text{ cm}^{-1}$  resolution. A path length of 1 mm was normally used. UV/vis absorption spectra were obtained in quartz cuvettes using a UNICAM UV-2 spectrophotometer, typically with a wavelength resolution of 1 nm. The estimated uncertainty in absorption maxima is  $\pm 2$  nm.
- Emission measurements were performed on a combined fluorescence lifetime and steady-state spectrometer (Edinburgh Instruments FLS920). Samples were thoroughly degassed using the freeze–pump–thaw technique, in specially modified  $1\text{ cm} \times 1\text{ cm}$  quartz cuvettes, and the optical density was adjusted to ca. 0.2 at the excitation wavelength. Steady-state emission and excitation
- (18) (a) Adams, H.; Alsindi, W.; Davies, G. M.; Duriska, M. B.; Easun, T. L.; Fenton, H.; Herrera, J.-M.; George, M. W.; Ronayne, K. L.; Sun, X.-Z.; Towrie, M.; Ward, M. D. *Dalton Trans.* **2006**, 39. (b) Herrera, J.-M.; Baca, S. G.; Adams, H.; Ward, M. D. *Polyhedron* **2006**, *25*, 869.
- (19) Elliott, M. C.; Hershenhart, E. J. *J. Am. Chem. Soc.* **1982**, *104*, 7519.

**Table 1.** UV/vis Absorption and Luminescence Data for the Complexes in This Study (Fluid Solution, Room Temperature)

compound	solvent	absorption				emission
		$\lambda_{\text{abs}}^1$ (nm)	$\lambda_{\text{abs}}^2$ (nm)	$\lambda_{\text{abs}}^3$ (nm)	$\lambda_{\text{abs}}^4$ (nm)	$\lambda_{\text{em}}$ (nm)
<b>1</b>	CH <sub>3</sub> CN	384 (2.6)	304 (3.6; sh)			687
<b>2</b>	CH <sub>3</sub> CN	585 (2.4)	418 (7.6)			<i>a</i>
<b>2</b>	D <sub>2</sub> O	437 (2.2)	342 (5.8)	257 (sh)		<i>a</i>
<b>3</b>	CH <sub>3</sub> CN	453 (12.9)	418 (10.3; sh)	400 (7.9)	360 (8.2), 330 (13.9)	648
<b>4</b>	DMF	480 (3.7)	350 (6.6)			<i>a</i>
<b>5</b>	CH <sub>3</sub> CN	685 (5.6)	628 (sh)	436 (20.7)		<i>a</i>
<b>5</b>	D <sub>2</sub> O	510 (3.8)	362 (12.7)			<i>a</i>
<b>6</b>	CH <sub>3</sub> CN	581 (6.5)	526 (6.4)	424 (22.9)	400 (20.5), 360 (13.5; sh)	774

<sup>a</sup> Nonluminescent under these conditions.

spectra were obtained with a xenon arc lamp as the excitation source and were corrected for detector sensitivity. Emission lifetime measurements were performed using the time-correlated single-photon counting technique, with a nanosecond dihydrogen flash lamp (repetition rate 40 kHz and pulse width ca. 2 ns) as the excitation source. The estimated uncertainty in emission maxima is  $\pm 2$  nm.

Cyclic voltammetry was performed using freshly distilled acetonitrile at a concentration of ca.  $1 \times 10^{-3}$  M with [nBu<sub>4</sub>N]-[PF<sub>6</sub>] as the supporting electrolyte. The potential was controlled with an Autolab PG-Stat 100 potentiostat operated by GPES 4.1 computer software. A solvent-saturated atmosphere of dinitrogen was used to degas the samples, and all scans were performed under this atmosphere. A single-compartment, three-electrode cell (volume ca. 5 mL) was used with a Pt disk working electrode, a Pt wire counter electrode, and an Ag/AgCl reference electrode, which is chemically isolated from the cell solution by a bridge tube containing an electrolyte solution and tipped with a porous vycor frit. Scan rates used were 100–500 mV s<sup>-1</sup>; redox potentials reported in the main text were recorded at 200 mV s<sup>-1</sup>. Potentials quoted are versus Ag/AgCl.

**TRIR Spectroscopy.** TRIR experiments were carried out using the PIRATE apparatus at the Central Laser Facility of the CCLRC Rutherford Appleton Laboratory. This apparatus was described in detail previously.<sup>20</sup> ps-TRIR setup: Part of the output from a 1 kHz, 800 nm, 150 fs, 2 mJ titanium-sapphire oscillator/regenerative amplifier (Spectra Physics Tsunami/Spitfire) was used to pump a white-light-continuum seeded  $\beta$ -BaB<sub>2</sub>O<sub>4</sub> optical parametric amplifier (OPA). The signal and idler produced by this OPA were difference frequency mixed in a type I AgGaS<sub>2</sub> crystal to generate tuneable mid-IR pulses (ca. 150 cm<sup>-1</sup> fwhm; 1  $\mu$ J), which were split to give probe and reference pulses with data points collected every 4–5 cm<sup>-1</sup>. Second-harmonic generation of the residual 800 nm light provided 400 nm pump pulses. Both the pump and probe pulses were focused to a diameter of 200–300  $\mu$ m in the sample. Changes in IR absorption at various pump-probe time delays were recorded by normalizing the outputs from a pair of 64-element MCT IR linear array detectors on a shot-by-shot basis. ns-TRIR spectra were obtained using a Nd:YAG laser (Advanced Optical Technology ACE) as the excitation source and the detection system detailed above.

## Results and Discussion

**Complexes under Investigation.** The mononuclear complexes **1–3** and dinuclear complexes **4–6** (see Chart 1) fall into three groups: complexes based on the {Re(CO)<sub>3</sub>Cl} fragment coordinated to bipyrimidine (**1** and **4**), complexes containing {Ru(CN)<sub>4</sub>}<sup>2-</sup> fragments coordinated to bipyrimidine (**2** and **5**), and complexes containing {Ru(bpyam)<sub>2</sub>}<sup>2+</sup>

fragments coordinated to bipyrimidine (**3** and **6**). For complexes **1**, **2**, **4**, and **5**, there is only one ligand (bpm) that can act as the electron acceptor in MLCT transitions, whereas **3** and **6** offer the additional possibility of MLCT excitation to either the terminal bpm ligands or the central bpm ligand, generating initially two different <sup>3</sup>MLCT states of which the higher energy is expected to convert to the lower energy one via an internal relaxation process. The anionic cyanoruthenate complexes **2** and **5** display strong negative solvatochromism, a feature that we and others have investigated in a range of complexes of this type<sup>17,18,21</sup> and which allows tuning of the MLCT excited states by altering the solvent environment of the complexes. In light of this, the physical properties of **2** and **5** have been recorded in D<sub>2</sub>O and CH<sub>3</sub>CN wherever possible. The neutral rhenium complexes **1** and **4** are insoluble in aqueous media and were examined only in CH<sub>3</sub>CN as the solvent. All of the complexes contain IR-active functional groups (carbonyl for **1** and **4**, cyanide for **2** and **5**, and amide C=O for **3** and **6**), which provided the basis for TRIR studies.

**Absorption and Luminescence Properties.** Electronic absorption spectra of the complexes are summarized in Table 1. In general, the lowest-energy absorptions correspond to metal  $\rightarrow$  bpm singlet metal-to-ligand charge-transfer (<sup>1</sup>MLCT) transitions because of the low-lying unoccupied  $\pi^*$  orbitals on the bpm ligand.<sup>10</sup> Although complexes **1**, **2**, **4**, and **5** are known, it is appropriate to summarize briefly their spectroscopic properties here to assist in understanding the new TRIR data presented later.

**(a) Complexes 1 and 4.** The two absorption bands at 304 and 384 nm for **1** in CH<sub>3</sub>CN correspond to Re  $\rightarrow$  bpm <sup>1</sup>MLCT transitions involving two low-lying unoccupied  $\pi^*$  bpm orbitals at similar energy.<sup>10c</sup> These transitions move to lower energy upon coordination of the second metal center, to 375 and 484 nm, respectively, in **4**.<sup>10b</sup> The luminescence of **1** in CH<sub>3</sub>CN at 298 K is weak but detectable at room temperature,<sup>22</sup> occurring at 687 nm, considerably red-shifted

(20) Towrie, M.; Grills, D. C.; Dyer, J.; Weinstein, J. A.; Matousek, P.; Barton, R.; Bailey, P. D.; Subramaniam, N.; Kwok, W. M.; Ma, C.; Phillips, D.; Parker, A. W.; George, M. W. *Appl. Spectrosc.* **2003**, *57*, 367.

(21) (a) Timpson, C. J.; Bignozzi, C. A.; Sullivan, B. P.; Kober, E. M.; Meyer, T. J. *J. Phys. Chem.* **1996**, *100*, 2915. (b) Herrera, J.-M.; Ward, M. D.; Adams, H.; Pope, S. J. A.; Faulkner, S. *Chem. Commun.* **2006**, 1851.

(22) Shavaleev, N. M.; Accorsi, G.; Virgili, D.; Bell, Z. R.; Lazarides, T.; Calogero, G.; Armaroli, N.; Ward, M. D. *Inorg. Chem.* **2005**, *44*, 61.

compared to  $[\text{Re}(\text{bpy})(\text{CO})_3\text{Cl}]$ .<sup>23</sup> The dinuclear complex **4** is nonluminescent in a  $\text{CH}_3\text{CN}$  solution (and also in the solid state and in glasses down to 4 K).<sup>10a</sup>

**(b) Complexes 2 and 5.** These complexes exhibit the expected strong negative solvatochromism due to specific donor–acceptor interactions between the cyanide lone pairs and surrounding solvent molecules, which results in higher MLCT energies in protic media.<sup>17,21a</sup> For **2**, the two  $\text{Ru} \rightarrow \text{bpm}$  <sup>1</sup>MLCT transitions are centered at 437 and 342 nm in  $\text{D}_2\text{O}$  and at 585 and 418 nm in  $\text{CH}_3\text{CN}$ . Again complexation of the second metal center to give dinuclear **5** reduces the energies of the unoccupied ligand orbitals and red-shifts the <sup>1</sup>MLCT absorptions, so in both  $\text{CH}_3\text{CN}$  and  $\text{D}_2\text{O}$  the  $\text{Ru} \rightarrow \text{bpm}$  <sup>1</sup>MLCT transitions of **5** are observed at lower energy than those of the mononuclear **2**.<sup>9a</sup> Intense structured features at higher energy are assigned to intraligand transitions and are largely independent of metal complexation. No luminescence was detected from either **2** or **5** in either solvent.

**(c) Complexes 3 and 6.** The absorption spectra of these complexes are only slightly affected by the solvent, with differences of a few nanometers in wavelength between related absorptions in  $\text{D}_2\text{O}$  and  $\text{CH}_3\text{CN}$ . More low-energy absorption bands are observed in comparison with the other complexes, owing to the presence of  $\text{Ru} \rightarrow \text{bpyam}$  <sup>1</sup>MLCT transitions in addition to the  $\text{Ru} \rightarrow \text{bpm}$  transitions. There are two transitions, at ca. 420 and 400 nm, whose positions do not vary significantly with either the solvent or nuclearity and, hence, are tentatively assigned to the  $\text{Ru} \rightarrow \text{bpyam}$  <sup>1</sup>MLCT transitions. The bands at ca. 450 and 330 nm in **3** are thought to correspond to those at 581 and 526 nm in the dinuclear **6** and are tentatively assigned to two  $\text{Ru} \rightarrow \text{bpm}$  <sup>1</sup>MLCT transitions. This is again consistent with (i) the presence of two different low-lying  $\pi^*$  bpm orbitals giving two <sup>1</sup>MLCT transitions to bpm and (ii) the reduction in energy of the bpm  $\pi^*$  orbitals upon complexation of a second metal to the bpm ligand.

The luminescence of **3** in  $\text{CH}_3\text{CN}$  is relatively intense at room temperature, resembling that of  $[\text{Ru}(\text{bpy})_3]^{2+}$ <sup>24</sup> with a broad structureless emission peak centered at 648 nm, which decays with a time constant of  $116 (\pm 10)$  ns. By comparison, the luminescence of **6** in  $\text{CH}_3\text{CN}$  is at lower energy (774 nm) and is much weaker and shorter-lived (7 ns from TRIR studies; see below), reflecting the stabilizing effect on the LUMO of the complexation of the second metal center to the bpm ligand.

**TRIR Studies.** Laser excitation at 400 nm is into a metal  $\rightarrow$  bpm <sup>1</sup>MLCT transition for complexes **1**, **2**, **4**, and **5** and into an overlapping set of  $\text{Ru} \rightarrow \text{bpm}$  and  $\text{Ru} \rightarrow \text{bpyam}$  <sup>1</sup>MLCT transitions for complex **3**. In complex **6**, excitation at 400 nm is primarily into a  $\text{Ru} \rightarrow \text{bpyam}$  <sup>1</sup>MLCT transition (vide supra).

**(a) Complexes 1 and 4.** Figure 1 shows the FTIR and ps-TRIR spectra obtained for **1** in a  $\text{CH}_3\text{CN}$  solution. The FTIR spectrum of **1** displays three  $\nu(\text{CO})$  bands. After laser

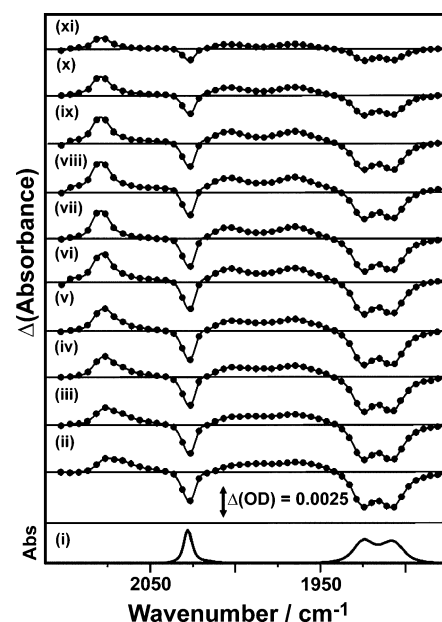


**Figure 1.** FTIR (i) and TRIR spectra of **1** in  $\text{CH}_3\text{CN}$  obtained (ii) 2 ps, (iii) 4 ps, (iv) 7.5 ps, (v) 10 ps, (vi) 20 ps, (vii) 50 ps, (viii) 100 ps, (ix) 200 ps, (x) 500 ps, and (xi) 1000 ps after 400 nm excitation.

excitation at 400 nm, all three shift to higher energy, which is typical for the <sup>3</sup>MLCT excited state of  $[\text{Re}(\text{CO})_3\text{Cl}(\text{diimine})]$  complexes.<sup>12a</sup> The excited state is initially formed vibrationally “hot” and cools over the first 20 ps, as evidenced by narrowing and slight blue-shifting of the transient bands over this time scale.<sup>25</sup> The excited-state bands decay at the same rate as the bleaches recover [ $\tau = 1.2 (\pm 0.1)$  ns]. This is significantly shorter than the excited-state lifetime of  $[\text{Re}(\text{bpy})(\text{CO})_3\text{Cl}]$ <sup>12a,23</sup> and consistent with the “energy-gap law”<sup>26</sup> and the lack of any significant luminescence from this complex.

FTIR and ps-TRIR spectra obtained for the dinuclear analogue **4** in a  $\text{CH}_3\text{CN}$  solution are shown in Figure 2. The FTIR spectrum of dinuclear **4** also displays three  $\nu(\text{CO})$  bands; the spectrum is comparable to that of **1**. Although there are two possible isomers of this complex with the chloride ligands either syn or anti to each other, the <sup>1</sup>H NMR spectrum shows a single set of resonances, indicating the presence of only one isomer. After laser excitation, the ps-TRIR spectrum yields two sets of three excited-state transient bands. One set is very similar to the transient carbonyl bands observed in the IR spectrum of the MLCT excited state of **1**, i.e., shifted to higher energy with respect to the ground state, and the other set of three bands is shifted to lower energy by  $15\text{--}35 \text{ cm}^{-1}$ , indicative of a metal center that has become more electron-rich. The positions of the bands shifted to lower energy are in good agreement with the IR bands of the reduced form of **4**, within which the added electron is localized on the central bpm ligand, obtained from optically transparent thin-layer electrode spectroelectrochemistry experiments (Figure 3). The presence of two sets of  $\nu(\text{CO})$  transients, one with a positive shift and one with a negative

(23) Worl, L. A.; Duesing, R.; Chen, P.; Della Ciana, L.; Meyer, T. J. *J. Chem. Soc., Dalton Trans.* **1991**, 849.

(24) Felix, F.; Ferguson, J.; Gudel, H. U.; Ludi, A. *J. Am. Chem. Soc.* **1980**, *102*, 4096.

(25) Dougherty, T. P.; Heilweil, E. J. *J. Chem. Phys.* **1994**, *100*, 4006.

(26) Caspar, J. V.; Kober, E. M.; Sullivan, B. P.; Meyer, T. J. *J. Am. Chem. Soc.* **1982**, *104*, 630.

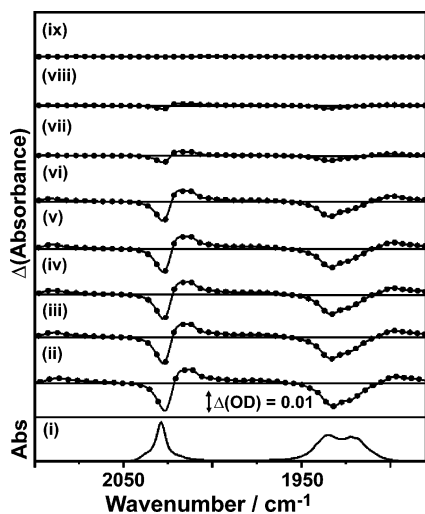


**Figure 2.** FTIR (i) and TRIR spectra of **4** in CH<sub>3</sub>CN obtained (ii) 2 ps, (iii) 4 ps, (iv) 7.5 ps, (v) 10 ps, (vi) 20 ps, (vii) 50 ps, (viii) 100 ps, and (ix) 200 ps after 400 nm excitation.

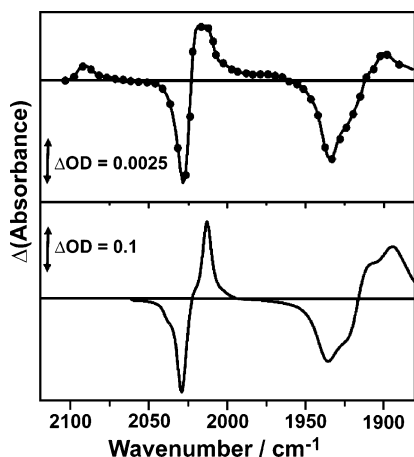


**Figure 3.** TRIR of **4** (top) and the FTIR difference spectrum obtained following electrochemical generation of the radical anion **4**<sup>•-</sup> (bottom), both in CH<sub>3</sub>CN.

shift compared to the ground state, has been observed previously for <sup>3</sup>MLCT states of dinuclear carbonyl complexes.<sup>15a-e</sup> The <sup>3</sup>MLCT excited state is accordingly best formulated as having an asymmetric charge distribution in the excited state, such that the transient structure may be written in the form [Re<sup>I</sup>(bpm<sup>•-</sup>)Re<sup>II</sup>]. This complex constitutes an example of an “excited-state mixed-valence” species<sup>14</sup> in which the valences are localized on the IR time scale and shows behavior similar to that of other dinuclear complexes containing {Re(CO)<sub>3</sub>} fragments connected by a polypyridine-type bridging ligand.<sup>15a-d</sup> The decay of the excited state [ $\tau = 46 (\pm 5)$  ps] is considerably shorter than that for mononuclear **1** in the same solvent ( $\tau = 1.2$  ns). A significant factor here is that the lower energy of the MLCT excited state for the dinuclear complex will be more readily quenched by molecular vibrations, resulting in a shorter-lived excited state, as predicted by the energy-gap law.<sup>26</sup> In addition, it has been suggested that the existence of a low-energy rhenium(0)–rhenium(II) excited state may provide an additional quenching pathway that does not exist for mononuclear **1**, although there appears to be no concrete evidence for this.<sup>10a</sup>

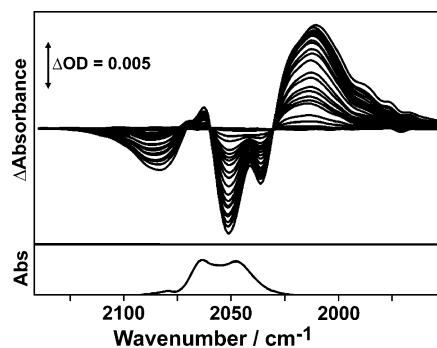


**Figure 4.** FTIR (bottom) and TRIR (top) spectra of **5** in CH<sub>3</sub>CN.  $\lambda_{\text{exc}} = 400$  nm; time delays shown are between 1 and 2000 ps.

(b) **Complexes 2 and 5.** TRIR investigations into the mononuclear complex **2** have been reported,<sup>18a</sup> the main relevant features are summarized here. Its FTIR spectrum exhibits four  $\nu(\text{CN})$  bands in both CH<sub>3</sub>CN and D<sub>2</sub>O. Three of these bands are at lower energy in the latter solvent; the fourth appears to be less solvent-sensitive. Only three bands can usually be resolved in our TRIR experiments. Following excitation, the parent bands bleach, a single major transient band is observed at higher energy, and the magnitude of the shift from the peak center of the major bleach component to the peak center of the major transient component can be used to compare the differences in the spectra. It can be seen that this shift is larger in D<sub>2</sub>O (49 cm<sup>-1</sup>) than in CH<sub>3</sub>CN (30 cm<sup>-1</sup>). This shift to higher energy can be interpreted in the same way as that for metal carbonyls, viz., a reduction in metal-to-cyanide  $\pi$ -back-bonding in the excited state, although it has recently been suggested that this interpretation is too simplistic and that the electrostatic consequences of the increase in charge on the central metal ion are also important.<sup>27</sup> The excited state decays much more rapidly in CH<sub>3</sub>CN [ $\tau = 250 (\pm 20)$  ps] than in D<sub>2</sub>O [ $\tau = 3.4 (\pm 0.3)$  ns]. The longer excited-state lifetime in D<sub>2</sub>O is due to a combination of two effects: increased hydrogen bonding of the cyanides with the solvent leads to an increased HOMO–LUMO energy gap in D<sub>2</sub>O compared to CH<sub>3</sub>CN,<sup>18a,b</sup> and the use of a deuterated solvent further attenuates the nonradiative deactivation pathways by lowering the energy of the relevant solvent vibrations.<sup>18a,28</sup>

Figure 4 shows the FTIR and ps-TRIR spectra obtained for dinuclear complex **5** in a CH<sub>3</sub>CN solution (top) and a D<sub>2</sub>O solution (bottom). The excited state again decays much faster in CH<sub>3</sub>CN [ $\tau = 65 (\pm 2)$  ps] than in D<sub>2</sub>O [ $\tau = 1200 (\pm 100)$  ps]. This is in keeping with the solvent dependence observed for mononuclear complex **2** and with diimine–cyanoruthenate complexes in general.<sup>18a</sup> These lifetime values are also considerably shorter than those of mononuclear **2** in the same solvents (cf. the discussion of the lifetimes of mononuclear **1** and dinuclear **4** above).

Comparison of the lifetime behavior of **1** and **4** vs **2** and **5** in CH<sub>3</sub>CN is interesting. Although in both cases the dinuclear complexes have a shorter lifetime than the corre-

(27) Kettle, S. F. A.; Aschero, G. L.; Diana, E.; Rossetti, R.; Stanghellini, P. L. *Inorg. Chem.* **2006**, *45*, 4928.

(28) Kovacs, M.; Horvath, A. *Inorg. Chim. Acta* **2002**, *335*, 69.

sponding mononuclear complexes, the difference is significantly less between **2** and **5** ( $\tau_2 \approx 3\tau_5$ ) than between **1** and **4** ( $\tau_1 \approx 26\tau_4$ ). Although the lifetime of both **2** and **5** in  $D_2O$  is much longer than that in  $CH_3CN$ , the same ratio of lifetimes is observed ( $\tau_2 \approx 3\tau_5$  in each solvent). This can be ascribed to the fact that the addition of a second  $\{Re(CO)_3Cl\}$  center (on changing from **1** to **4**) reduces the lowest  $^1MLCT$  absorption by  $5400\text{ cm}^{-1}$ , whereas the addition of a second  $\{Ru(CN)_4\}^{2-}$  center (on changing from **2** to **5**) has a smaller effect on the lowest  $MLCT$  state, reducing the lowest  $^1MLCT$  absorption by only  $3300\text{ cm}^{-1}$  in water. Consequently, there is a bigger difference between the LUMO energies of **1** and **4** than between those of **2** and **5**, and the energy-gap law accordingly predicts a bigger drop in the excited-state lifetime between **1** and **4** on the basis of  $^3MLCT$  energies. It is likely that the weaker stabilizing effect on the bpm LUMO of an additional  $\{Ru(CN)_4\}^{2-}$  unit compared to an additional  $\{Re(CO)_3Cl\}$  unit is because the former is a poorer  $\pi$  acceptor on account of its  $2-$  charge.

In complex **5**, there are, in both solvents, two sets of transient  $\nu(CN)$  bands in the TRIR spectrum; one to higher energy than the ground state and one to lower energy. This is exactly similar to what we observed in **4** and indicates that the excited state is again an asymmetric (i.e., valence-localized) mixed-valence species  $[(NC)_4Ru^{II}(\mu\text{-bpm}^{\bullet-})\text{-}Ru^{III}(CN)_4]^{4-}$  on the IR time scale, i.e., with spectroscopically distinct  $\{Ru(CN)_4\}$  termini. The oxidized metal center has its transient  $\nu(CN)$  bands at higher energy, whereas the “spectator” ruthenium(II) center becomes more electron-rich because of the electron being pushed toward it, such that its transient  $\nu(CN)$  bands are at lower energy because of increased Ru–CN back-bonding. It is noticeable, however, that the relative intensities of the high- and low-energy transient bands are very different in the two solvents. In  $CH_3CN$ , the high-energy transient is very weak (almost lost under the bleaches of the parent  $\nu(CN)$  manifold), whereas the low-energy transient is relatively intense and dominates the spectrum. In  $D_2O$ , the same trend occurs but to a much smaller extent, with the high-energy transient now being clearly visible and the low-energy transient, while still the more intense of the two, being weaker than that in  $CH_3CN$ . The general pattern of weak high-energy  $\nu(CN)$  transient bands compared to intense low-energy  $\nu(CN)$  transient bands is consistent with simple expectations based on how the charge distribution in the excited state will affect the C–N dipoles,<sup>29</sup> but the nature of the solvent clearly also has a substantial effect.<sup>30</sup>

UV/vis and IR spectroelectrochemistry for complexes **2** and **5** was unsuccessful for all oxidative and reductive couples because of the chemical irreversibility of the processes on the long time scale of a spectroelectrochemistry experiment.

**(c) Complexes 3 and 6.** Figure 5 shows the ps-TRIR spectra obtained for mononuclear complex **3** in a  $D_2O$  solution. The FTIR spectrum of **3** exhibits a single amide  $\nu(CO)$  band in both  $D_2O$  and  $CH_3CN$ , at  $1617$  and  $1641\text{ cm}^{-1}$ , respectively, and a weak band at ca.  $1580\text{ cm}^{-1}$ , which

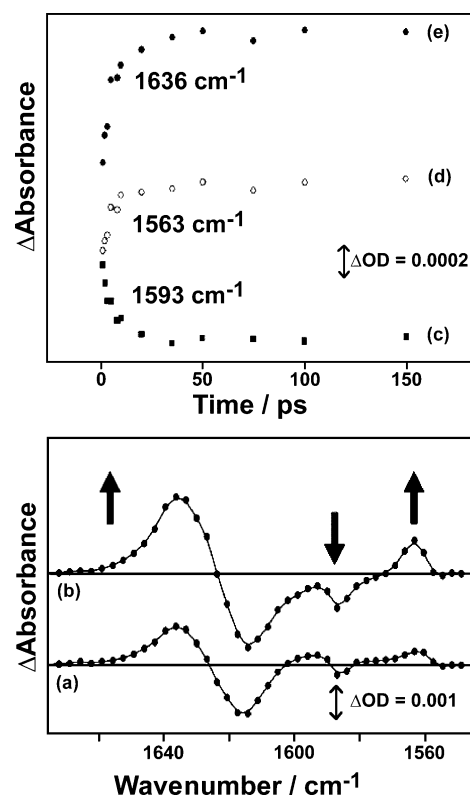


**Figure 5.** TRIR spectra of **3** in  $D_2O$  obtained (a) 1 ps and (b) 100 ps after 400 nm excitation. TRIR kinetic traces of transients recorded at (c)  $1593\text{ cm}^{-1}$ , (d)  $1563\text{ cm}^{-1}$ , and (e)  $1636\text{ cm}^{-1}$ .

is solvent-independent and is assigned to a vibrational mode of bipyrimidine.

Following 400 nm laser excitation in  $D_2O$ , the TRIR spectrum of **3** exhibits several features. The parent  $\nu(CO)$  amide band is bleached, and two transient bands are observed: one at higher energy ( $1636\text{ cm}^{-1}$ ) and one at lower energy ( $1593\text{ cm}^{-1}$ ). This is because initial excitation is nonselective (cf. the electronic absorption spectrum *vide supra*) such that both  $[(bpyam)(bpyam^{\bullet-})Ru^{III}(bpm)]^{2+}$  [hereafter  $MLCT(bpyam\text{-}3)$ ] and  $[(bpyam)_2Ru^{III}(bpm^{\bullet-})]^{2+}$  [hereafter  $MLCT(bpm\text{-}3)$ ] excited states are formed in the first instance. The higher-energy transient, which corresponds to

(29) It is interesting that the lower-energy transient band associated with the “spectating”  $\{Ru^{II}(CN)_4\}$  terminus has (in both  $CH_3CN$  and  $D_2O$ ) a much higher intensity than the weak high-energy transient band associated with the  $\{Ru^{III}(CN)_4\}$  terminus. This can be accounted for on the basis of a change in the dipole moment of the  $C\equiv N$  bonds following charge redistribution in the excited state (ref 27). The increase in the electron density at the spectating ruthenium center in the excited state leads to an increase in the negative charge on the carbon atoms and hence an increase in the effective dipole moment of the  $C\equiv N$  oscillators, giving more intense  $\nu(CN)$  bands. The converse is true for the transiently oxidized ruthenium center, whose  $\nu(CN)$  band in the excited state is correspondingly weak because transient oxidation of the metal center reduces the partial negative charge on carbon and hence reduces the  $C\equiv N$  dipole.

(30) There are two quite different contributions to the solvent-dependent behavior of this type of complex: (i) the change in the dipole moment on going from the ground to excited state, which will affect solvation by any dipolar solvents; (ii) the presence of specific hydrogen-bonding interactions between cyanides and protic solvents, which change between the ground and excited states (see ref 17). The extent to which each of these factors contributes to the change in the dipole moment of the  $C\text{--}N$  oscillators on going from the ground to excited state, and hence the intensity of the transient bands in the TRIR difference spectra, is a complex issue and is beyond the scope of this paper.

a decrease in the electron density on the bpyam ligands, is consistent with the formation of the MLCT(bpm-3) excited state. The lower-energy transient, which corresponds to an increase in the electron density on the bpyam ligands (and partial population of the bpyam LUMO, which has C=O antibonding character), is conversely consistent with the formation of the MLCT(bpyam-3) excited state.

The behavior of these two transients allows us to monitor the fast interconversion of the higher-lying MLCT(bpyam-3) excited state to the lower-lying MLCT(bpm-3) excited state. The higher-energy transient band grows in with a time constant of 7 ( $\pm$ 2) ps (Figure 5) and then decays at the same rate as the recovery of the parent bleach, with a time constant of 60 ( $\pm$ 5) ns. The 7 ps grow-in corresponds to the formation of the MLCT(bpm-3) state from the higher-energy MLCT-(bpyam-3) excited state; i.e., relaxation of the higher-lying bpyam-based <sup>3</sup>MLCT state to the lower-lying bpm-based <sup>3</sup>MLCT state occurs with a lifetime of 7 ( $\pm$ 2) ps. The subsequent 60 ns decay corresponds to the lifetime of the MLCT(bpm-3) lowest excited state under these conditions (cf. the value of 116 ns determined using luminescence methods). (This discrepancy is likely due to the much higher analyte concentrations required for TRIR experiments, which will lead to self-quenching, an effect that has been observed previously.<sup>31</sup> Another possible reason for the shorter lifetimes observed by TRIR measurements compared to luminescence measurements is the inferior degassing regime that is used during the PIRATE TRIR experiments. Both of these factors will result in shorter <sup>3</sup>MLCT lifetimes under the conditions of TRIR measurements compared to luminescence measurements.) Consistent with this interpretation, the low-energy transient [arising from the MLCT(bpyam-3) excited state] decays at the same rate as the transient for MLCT(bpm-3) grows in (Figure 5). This is consistent with the formation of a short-lived MLCT(bpyam-3) state, which is partly populated by the nonselective 400 nm excitation and quickly converts to the lower-energy MLCT(bpm-3) state. The bpm-based vibration at 1585 cm<sup>-1</sup> is also bleached on excitation, with a transient appearing to lower energy (1560 cm<sup>-1</sup>) due to the formation of the MLCT(bpm-3) state, in which the bpm ligand is reduced. Recovery of the parent band and the decay of the transient both occur with the same time constant (60 ns) as that observed for the higher-energy amide transient band; hence, they are also monitoring the decay of the MLCT(bpm-3) excited state.

In CH<sub>3</sub>CN, the TRIR spectra of **3** exhibit a similar bleach of the main  $\nu$ (CO) amide band following 400 nm excitation. Transient  $\nu$ (CO) bands are seen at both lower and higher energy than the ground state (at 1652 and 1623 cm<sup>-1</sup>), consistent with near-simultaneous population of both MLCT-(bpyam-3) and MLCT(bpm-3) excited states. The lower-energy  $\nu$ (CO) transient again overlaps with the bleach of the ground-state band and is assigned to the formation of MLCT(bpyam-3). The IR transient band associated with MLCT(bpyam-3) decays (4.0  $\pm$  1.5 ps) at the same rate as MLCT(bpm-3) is formed (6.0  $\pm$  2.4 ps). MLCT(bpm-3) then

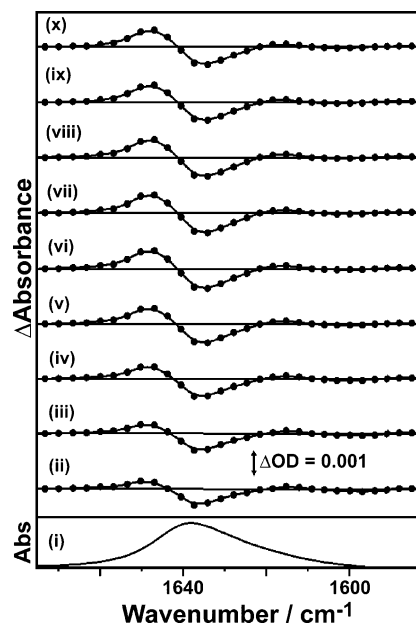


**Figure 6.** FTIR (i) and TRIR spectra of **6** in CH<sub>3</sub>CN obtained (ii) 2 ps, (iii) 5 ps, (iv) 10 ps, (v) 20 ps, (vi) 50 ps, (vii) 100 ps, (viii) 200 ps, (ix) 500 ps, and (x) 750 ps after 400 nm excitation.

decays to reform the ground state with  $\tau = 97 (\pm 3)$  ns. Similar to the results described in D<sub>2</sub>O, the bpm-based ground-state band at 1580 cm<sup>-1</sup> is bleached and a lower-energy transient grows in at 1559 cm<sup>-1</sup> and then decays with the same lifetime (97 ns) as that of the higher-energy transient amide  $\nu$ (CO) band. Thus, in both solvents, we are observing interconversion of the higher-lying MLCT(bpyam-3) state to the lower-lying MLCT(bpm-3) state on a similar time scale.

Figure 6 shows the FTIR and ps-TRIR spectra obtained for dinuclear complex **6** in a CH<sub>3</sub>CN solution. The FTIR spectrum of **6** is similar to that of the mononuclear analogue **3**, in that a single amide  $\nu$ (CO) band is seen in both solvents, at 1615 cm<sup>-1</sup> and 1636 cm<sup>-1</sup> in D<sub>2</sub>O and CH<sub>3</sub>CN, respectively. Upon 400 nm excitation, the parent  $\nu$ (CO) band is bleached and a transient band is observed at higher energy. In both solvents, the shift to higher energy is small (20–40 cm<sup>-1</sup>) and both the bleach and transient are broad and overlapped, making deconvolution more difficult. Initial excitation is nonselective so both [(bpyam)(bpyam<sup>-</sup>)-Ru<sup>III</sup>(bpm)Ru<sup>II</sup>(bpyam)<sub>2</sub>]<sup>4+</sup> [hereafter MLCT(bpyam-6)] and [(bpyam)<sub>2</sub>Ru<sup>III</sup>(bpm<sup>-</sup>)Ru<sup>II</sup>(bpyam)<sub>2</sub>]<sup>4+</sup> [hereafter MLCT-(bpm-6)] triplet excited states are expected on the picosecond time scale, with the latter being significantly lower in energy (as demonstrated by UV/vis spectroscopy, vide supra).

As with the mononuclear complex **3**, the transient  $\nu$ (CO) band that is shifted to higher energy can be ascribed to, and can be used to monitor the formation and decay of, the MLCT(bpm-6) excited state. In D<sub>2</sub>O, this transient grows in with a time constant of 9 ( $\pm$ 1) ps and then decays synchronously with the recovery of the parent bleach with a lifetime of 6 ( $\pm$ 2) ns. Similarly, in CH<sub>3</sub>CN, the higher energy  $\nu$ (CO) MLCT(bpm-6) transient grows in and then decays synchronously with the parent bleach recovery with a lifetime of 7 ( $\pm$ 1) ns. In both cases, this behavior is consistent with

(31) Glyn, P.; George, M. W.; Hodges, P. M.; Turner, J. J. *J. Chem. Soc., Chem. Commun.* **1989**, 1655



fast (picosecond time scale) internal conversion of the higher-lying MLCT(bpyam-**6**) state to the lower-lying MLCT(bpm-**6**) state, formally by internal electron transfer from (bpyam)<sup>−</sup> to bpm, followed by a slower decay of the MLCT(bpm-**6**) state to the ground state on the nanosecond time scale. There is some evidence for a short-lived lower-energy  $\nu(\text{CO})$  transient in both solvents from inspection of the parent bleach profile and kinetics, which we assign to initial generation of the MLCT(bpyam-**6**) state by nonselective excitation at 400 nm. This is expected by comparison with the mononuclear complex. In both solvents, the bands assigned to MLCT-(bpyam-**6**) decay rapidly ( $7 \pm 2$  ps). However, a much clearer lower-energy  $\nu(\text{CO})$  band is observed in CH<sub>3</sub>CN, at a slightly lower energy ( $1615 \text{ cm}^{-1}$ ), which persists on the nanosecond time scale and decays at the same rate as the MLCT(bpm-**6**) excited state, and this may be due to a broader excited-state transient band overlapping the parent bleach.

### Conclusions

In all of these complexes, the TRIR spectra have clearly demonstrated the metal  $\rightarrow$  bpm <sup>3</sup>MLCT nature of the lowest excited states, with the excited state being lower in energy and shorter-lived in the dinuclear complexes compared to the related mononuclear ones, and we have been able to determine excited-state dynamics for several complexes that are nonluminescent. The main conclusions are as follows:

(i) In the dinuclear complexes **4** (in CH<sub>3</sub>CN) and **5** (in both CH<sub>3</sub>CN and D<sub>2</sub>O), it is clear that the metal  $\rightarrow$  bpm-

based MLCT excited states are best represented as localized on the IR time scale, i.e., two sets of transient IR bands are observed, at higher *and* lower energy than the parent bleach, indicative of spectroscopically distinct metal centers on the IR time scale; the bands to higher energy are in the same positions as those of the corresponding mononuclear complex.

(ii) In complexes **3** and **6**, there are two possible types of MLCT transition, Ru  $\rightarrow$  bpm (to the bridging bpm ligand) and Ru  $\rightarrow$  bpyam (to the terminal ligands). Of these, the former is lower in energy. Excitation at 400 nm results in nonselective excitation of the complex into both excited states, but we can detect using TRIR the rapid decay of the Ru  $\rightarrow$  bpyam MLCT state to the lower-lying Ru  $\rightarrow$  bpm state on the picosecond time scale before the much slower decay of the Ru  $\rightarrow$  bpm state on the nanosecond time scale. These changes can be followed using both the amide carbonyl reporter groups on the terminal ligands and a bipyrimidine-based vibration.

Photophysical studies on related heterodinuclear bipyrimidine-bridged complexes are in progress and will be reported later.

**Acknowledgment.** We thank the EPSRC for financial support (Grants GR/S50724 and GR/S50731). We thank the Council for the Central Laboratory of the Research Councils for funding access to the Central Laser Facility.

IC0623112